PRELIMINARY THERMODYNAMIC ASESSEMENT OF A REFRIGERATION SYSTEM WITH A PCM BASED DEFROSTING
/
EVALUAREA TERMODINAMICĂ PRELIMINARĂ A UNUI SISTEM FRIGORIFIC CU DEGIVRARE PE BAZĂ DE PCM

Valentin APOSTOL[1)], Horatiu POP *[1)], Tudor PRISECARU[1)], Claudia IONITA[1)], Jamal AL DOURI[1)]
Adrian CHIRIAC*[1,2)], Cornel Constantin PAVEL[1)]
[1)] Faculty of Mechanical Engineering and Mechatronics, National University of Science and Technology POLITEHNICA Bucharest / Romania.
[2)] Academy of Romanian Scientists, Ilfov 3, 050044 Bucharest, Romania
Tel: +40744903488; E-mail: horatiu.pop@upb.ro; Tel: +40721882659; E-mail: gabriel.chiriac@upb.ro
Corresponding authors: Horaţiu POP; Adrian CHIRIAC
DOI: https://doi.org/10.35633/inmateh-75-44

Keywords: *vapor compression refrigeration, phase change material, evaporator, defrosting, thermal energy storage*

ABSTRACT
This article presents a preliminary thermodynamic evaluation of a vapor compression refrigeration system (VCRS) using phase change materials (PCM) for defrosting. The objective of this study was to highlight the potential of heat recovery during the operation of the VCRS and its subsequent use in the defrosting process. The system was analyzed energetically, considering both the cooling and defrosting cycles using PCM-RT 35 HC. Input data are given, and they were experimentally measured on a VCRS installed in a freezing chamber located in the university campus. The analysis includes the following refrigerants: R32, R404A, R134a, R290, R600a, R600, R1234yf, and R1234ze(E). The results indicate that as the defrosting time increases, the refrigerant flow rate required for PCM-based defrosting decreases. Furthermore, it was observed that R600 requires the smallest refrigerant flow rate for the defrosting process, while R404A requires the highest to defrost the same mass of ice. The analysis revealed that R32 is the most suitable refrigerant for PCM-based defrosting, followed by wet or dry refrigerants (R404A, R134a, R290) and, finally, isentropic refrigerants (R600, R600a, R1234yf, R1234ze(E)). Additionally, it is noted that as the condensing temperature increased, the recoverable heat increased for R32, R404A, R134a, and R290, but decreased for isentropic refrigerants such as R600a, R600, R1234yf, and R1234ze(E). This analysis was conducted using a computational model implemented in the Engineering Equation Solver software.

REZUMAT
Acest articol prezintă o evaluare termodinamică preliminară a unui sistem frigorific cu comprimare mecanica de vapori (IFV) cu degivrare pe bază de materiale cu schimbare de fază (MSF). Scopul acestei lucrări a fost acela de a evidenția posibilitățile de recuperare a căldurii în timpul funcționării sistemului IFV si utilizarea ulterioară a acesteia in procesul de degivrare. Sistemul a fost analizat din punct de vedere energetic atât pentru ciclul de răcire cât și pentru cel de degivrare cu MSF-RT 35 HC. Datele de intrare au fost măsurate experimental pe un sistem IFV ce echipează o cameră de congelare existentă în campusul universitar. Sunt luați în considerare agenții frigorifici: R32, R404A, R134a, R290a R600a, R600, R1234yf si R1234ze(E). Rezultatele arată că dacă timpul de degivrare creste, debitul de agent frigorific necesar degivrării cu MSF, scade. De asemenea, se observă că în cazul agentului frigorific R600 s-a utilizat cel mai mic debit de agent frigorific pentru degivrare iar in cazul lui R404A, cel mai mare debit, pentru a degivra aceeași masă de gheață. Din analiză se constată că freonul R32 se pretează cel mai bine în cazul degivrării cu MSF urmat de freonii umezi sau uscați: R404A, R134a, R290 și în final de freonii izentropici: R600, R600a, R1234yf, R1234ze(E). Se constată de asemenea că odată cu creșterea temperaturii de condensare crește căldura recuperată în cazul lui R32, R404A, R134a, R290a și scade în cazul agenților frigorifici isentropici: R600a, R600, R1234yf si R1234ze(E). Această analiză s-a realizat folosind un model computerizat în software-ul Engineering Equation Solver.

Valentin APOSTOL, Prof. Ph. D. Eng.; Horatiu POP Assoc. Prof. Ph.D.Eng; Tudor PRISECARU Prof. Ph. D. Eng;
Claudia IONITA, Assoc.Prof. Ph.D.Eng.; Jamal Al Douri. Ph.D. Student; Adrian CHIRIAC, Ph.D. Student; Cornel Constantin PAVEL, Ph.D. Student

INTRODUCTION

Significant greenhouse gas emissions are released into the atmosphere due to the extensive use of fossil fuels and industrial activities. Heating, ventilation, air-conditioning, and refrigeration (HVAC-R) systems that operate on the vapor compression refrigeration (VCR) cycle contribute substantially to these emissions. Depending on the country, HVAC-R systems account for 16% to 50% of a building's total energy consumption (*Hepbasli, 2012*) and approximately 33% of overall greenhouse gas emissions (*Kharseh, et al., 2014*). Greenhouse gas emissions from VCR systems can be divided into direct and indirect sources. Direct emissions, which result from refrigerant leaks, represent about 20% of the total, while indirect emissions, due to electricity consumption, equipment manufacturing, cooler production, defrost system, and material recycling, constitute the remaining 80% (*Ragıp, et al., 2023*).

Refrigeration systems are a key component of the food industry. The most widely used refrigeration systems are the ones with vapor compression. A significant challenge for vapor compression refrigeration systems is the formation of ice on evaporator tubes, which poses a major operational issue. Ice formation begins when the surface temperature of the evaporator drops below both the freezing point of water and the dew point of the air, causing water vapor to condensate on the cold surface of the heat exchanger due to temperature differences. The water vapors that will eventually form the ice layer on the evaporator come from the food itself, from the moist air that enters the cold room when the door is opened or from other sources specific to each application Relative humidity (RH) of the air inside the cold room also plays a crucial role in the ice formation process *(Mohammed, et al., 2017*).

The frost layer increases the thermal resistance between the air and the refrigerant, resulting in a decrease in cooling capacity. Additionally, the cooling capacity is further diminished due to a reduction in air-side volumetric flow. This occurs because the hydraulic diameter of the flow channel decreases while fan power remains constant (*Le Gall et al., 1997*). Consequently, both the refrigeration system's cooling capacity and its coefficient of performance (COP) are adversely affected (*Al-Douri et al., 2024*). Therefore, periodic defrosting is necessary.

As highlighted by *Zhi-Ling et al., (2024),* previous experimental studies evaluating defrosting heat supply in case of reverse cycle method indicate that 71% to 80% of the total heat required for defrosting is sourced from the indoor heat exchanger.

The most used defrosting methods for refrigeration systems have been detailed in the authors' previous research (*Al-Douri et al., 2023*)**.** The defrosting method chosen for the given application has an influence on the air parameters (temperature, humidity) inside the refrigerating enclosure. The air parameters have a direct influence on the food products' quality. A defrost method based on a high operating temperature as electric defrosting for example, has as consequence a higher temperature inside the refrigerating enclosure at the end of the defrosting process. A defrosting method based on a low operating temperature like air defrosting for example has as consequence an increase in relative humidity inside of the refrigerating enclosure which can directly influence the quality of the food products. The PCM based defrosting method has a moderate operating temperature being suitable for applications from the food preservation industry. The current study focuses on an in-depth analysis of defrosting methods that employ phase change materials (PCM). Although most research in this field has been conducted at the level of heat pumps, the PCM approach has been investigated for its potential application to thermal energy storage (TES)-based defrosting methods in industrial refrigeration systems and beyond. According to the literature, TES-based defrosting methods are classified based on different energy sources into three categories: discharge heat storage, condensing heat storage, and subcooling heat storage.

For instance, to address the decline in heating capacity when the indoor heat exchanger is inactive, Wang et al. proposed operating the condenser and outdoor heat exchanger in parallel during defrosting mode. This configuration enables the PCM-HE to serve as a heat source for both space heating and defrosting. *Zhang et al., (2014*), demonstrated that heat dissipated from the compressor outlet of an air source heat pump, stored in the PCM-HE, can effectively melt frost on the outdoor coil. A similar discharge heat storage-based defrosting method has also been applied to air-cooled household refrigerators (*Dobre et al., 2024*; *Zhongbao, et al., 2018*).

In their work, *Jian-kai et al., (2011),* conducted an experimental comparison between the energy storage-based reverse cycle defrosting method and the traditional defrosting method for an air source heat pump. Under identical experimental conditions, the energy storage-based method reduced defrosting time by 60% and defrosting energy consumption by 48.1%.

Also, *Xin et al., (2021),* reported that PCM-HEs could store sufficient energy during the heating phase and release it to melt and evaporate frost during the defrosting phase for a heat pump. Similarly, *Zhaozhong et al., (2023),* demonstrated that for a split-air source heat pump (ASHP) unit utilizing phase change energy storage technology, the defrosting time could be shortened by 71.4–80.5%.

Zhang et al., (2014), also experimentally investigated the defrosting performance of a novel split-ASHP unit, where the compressor was encased in a PCM-HE to store dissipated heat. This innovative defrosting approach reduced energy consumption by 27.9% compared to the standard reverse cycle defrosting (SRCD) method (*Yang et al., 2019*).

Another experiment was conducted by *Miryam, et al., (2024),* who utilized heat from the discharge of a heat pump compressor, stored in a PCM heat exchanger. During the defrosting process, the refrigerant passes through the PCM heat exchanger, vaporizes, and is then directed to the system's evaporator to remove the frost.

Zhongbao et al., (2017), performed an experimental study on defrosting methods using TES in a household refrigerator, comparing it with electric resistance defrosting. The experimental results demonstrated that the thermal storage defrosting system could reduce power consumption by 71% compared to the original electric heater defrosting method.

Overall, the energy storage defrosting method is one of the most promising ways to solve the frosting problem of the refrigeration systems.

MATERIALS AND METHODS

System description

The refrigeration system operates in cooling mode for 5,5 h. In this time interval a specific amount of ice is deposited on the evaporator coil. This amount of ice will be removed in the defrosting interval of 0,5 hours.

Functional parameters are presented in Table 1.

Table 1

VCRS characteristics

Parameter	Value	Parameter	Value
Evaporating temperature t_o	-30°C	Cooling time $\tau_{cooling}$	5.5 hours
Condensing temperature t_c	33°C	Ice mass m_{ice}	1.4 kg
Cooling capacity $\dot{Q}_o$	4.5 kW	Heat storage capacity PCM RT 35-HC λ_{PCM}	240 kJ/kg
Defrosting time $\tau_{defrost}$	0.5 hours	Heat storage capacity Ice λ_{ice}	330 kJ/kg
Number of defrosts *n*	4	Pressure difference from p_8 to p_6, Δp	0.6 bar

The schematic and operating cycle of the VCRS are presented in Fig. 1 (a) and (b) respectively.

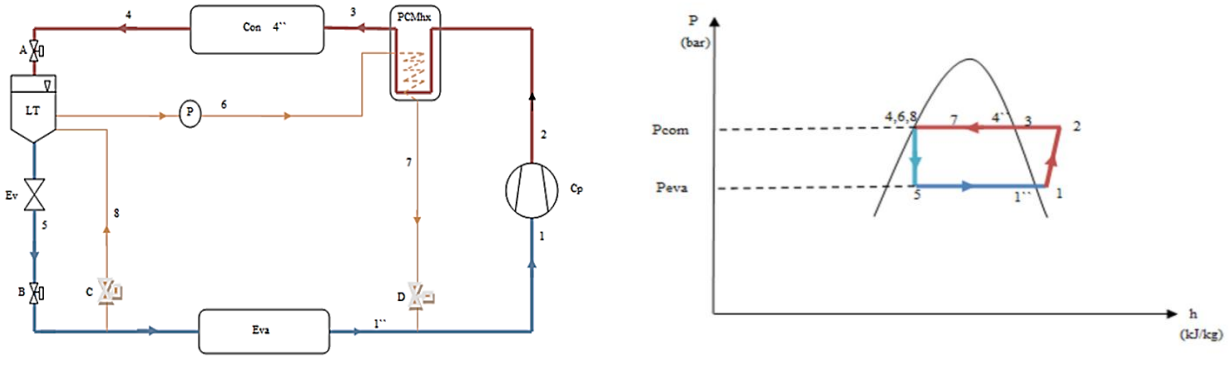

(a) **(b)**

Fig. 1 - The schematic and operating cycle of the VCRS

(a) - Schematic view of the VCRS system with PCM; (b)- Thermodynamic cycle if the VCR system with PCM;

The authors' previous work (*Al-Douri et al., 2023*) presented an experimental study on the use of a PCM heat exchanger for defrosting the evaporator of a refrigeration system installed in the CG 005 room at the National University of Science and Technology POLITEHNICA Bucharest - Faculty of Mechanical Engineering and Mechatronics, Department of Engineering Thermodynamics. The study investigated the impact of several PCM types of SP 31, RT 35 HC, RT 54 HC, and SP 50 on the energy performance of the vapor-compression refrigeration system (VCR) for various refrigerants. The results demonstrated that RT 35 HC was the most suitable PCM, as the same amount of thermal energy was stored for a significantly smaller PCM mass compared to the other materials analyzed.

In the present work, the same refrigeration system with RT 35 HC-based PCM defrosting is analyzed, focusing on different aspects compared to the previous study.

Mathematical model

The evaporative pressure $p_{eva.}$ [bar], the condensing pressure $p_{con.}$[bar], superheating degree Δt_{sh} are determined experimentally. With these values, the following thermodynamic states of the refrigerant can be determined:

$$\begin{aligned}
&State\ 1`` \rightarrow p_{eva.}\ \Omega\ x=1 \rightarrow t_{1''};\ h_{1''};\ v_{1''};\ s_{1''}\\
&State\ 1 \rightarrow p_{eva}\ \Omega\ (t_1=t_{1''}+\Delta t_{sh}) \rightarrow h_1;\ v_1;\ s_1\\
&State\ 2 \rightarrow p_{con}\ \Omega\ (s_1=s_2) \rightarrow t_2;\ h_2;\ v_2\\
&State\ 3 \rightarrow p_{con}\ \Omega\ (t_3=t_c+\Delta t_{rec}) \rightarrow h_3;\ v_3;\ s_3\\
&State\ 4 \rightarrow p_{con}\ \Omega\ x=0 \rightarrow t_4;\ h_4;\ v_4;\ s_4\\
&State\ 8 \rightarrow p_{con}\ \Omega\ x=0 \rightarrow t_8;\ h_8;\ v_8\\
&State\ 6 \rightarrow p_{con}+\Delta p\ \Omega\ (h_6=h_8+|l_{8\text{-}6}|) \rightarrow t_6;\ h_6;\ v_6;\ s_6;\ p_6\\
&State\ 5 \rightarrow p_{eva}\ \Omega\ (h_5=h_6) \rightarrow t_5;\ v_5;\ s_5\\
&State\ 7 \rightarrow p_{con}+\Delta p\ \Omega\ x_7=0.7 \rightarrow t_7;\ h_7;\ v_7;\ s_7
\end{aligned} \tag{1}$$

where Δp is the rise of pressure from condensing pressure needed to circulate the liquid refrigerant on the defrosting loop, p_6 is liquid refrigerant pressure at the inlet of the PCMhx given by the defrost pump and p_{con} is the condensing pressure. Also, l_{8-6} represents the specific work of the defrost pump.

In eq. (1) the specific work required by the circulation pump is given by: $|l_{8\text{-}6}| = v_8 \cdot \Delta p$ and the refrigerant quality in state 7 is imposed $x_7=0.7$.

The mass flow rate of refrigerant $\dot{m}$ can be written:

$$\dot{m} = \dot{Q}_0 / q_0 \tag{2}$$

$$q_0 = h_{1"} - h_5 \tag{3}$$

where: $\dot{Q}_0$ is the cooling capacity of the system and q_0 is the specific cooling capacity.

$$\tau_{between\ defrost} = (24/n) \cdot 3600 \tag{4}$$

$$\tau_{defrost} = 30\,\text{min} \tag{5}$$

$$\tau_{cooling} = \tau_{between\ defrost} - \tau_{defrost} \tag{6}$$

where $\tau_{between\ defrost}$ is the time between 2 consecutive defrost cycles, $\tau_{defrost}$ is the time when the system is in defrost mode and $\tau_{cooling}$ is the time period when the system is in cooling mode, all three being in seconds.

In Eq. (4), n represents the number of defrosts that take place in 24 hours.

$$\dot{Q}_{recovery} = \dot{m} \cdot (h_2 - h_3) \tag{7}$$

$$Q_{recovery} = \dot{Q}_{recovery} \cdot \tau_{cooling} \tag{8}$$

$$\lambda_{PCM} = 240\ {}^{kJ}\!/_{kg} \tag{9}$$

where $\dot{Q}_{recovery}$ is the heat flux that can be recovered from the refrigerant in the desuperheating process 2-3, $Q_{recovery}$ being the actual heat that can be recovered and λ_{PCM} is the heat storage capacity of PCM:

$$Q_{ice} = m_{ice} \cdot (c_{ice} \cdot (0 - t_{ice}) + \lambda_{ice}) \quad (10)$$

$$m_{ice} = 1.4\,kg \quad (11)$$

$$c_{ice} = 2.09\ {}^{kJ}\!/\!_{kg \cdot K} \quad (12)$$

$$t_{ice} = t_0 \quad (13)$$

$$\lambda_{ice} = 330\ {}^{kJ}\!/\!_{kg} \quad (14)$$

where Q_{ice} is the heat needed to melt the specific quantity of ice, (m_{ice}), c_{ice} is the specific heat of ice, t_{ice} represents the temperature of ice, which was taken equal to the evaporating temperature and λ_{ice} is the heat storage capacity for ice.

$$Q_{PCM} = m_{PCM} \cdot \lambda_{PCM} \quad (15)$$

$$Q_{PCM} = Q_{ice} \quad (16)$$

where Q_{PCM} is the heat that the mass of PCM (m_{PCM}) can absorb during defrosting period.

$$\dot{Q}_{ice} = Q_{ice} / \tau_{defrost} \quad (17)$$

$$\dot{Q}_{ice} = \dot{m}_{defrost} \cdot (h_7 - h_8) \quad (18)$$

where $\dot{Q}_{ice}$ is the heat flux that can be absorbed in time $\tau_{defrost}$, h_7 and h_8 are the specific enthalpies at the exit and inlet of the evaporator during the defrost period [kJ/kg].

$$P_{cp} = \dot{m} \cdot (h_2 - h_1) \quad (19)$$

$$P_{p1} = |l_{8-6}| \cdot \dot{m}_{defrost} \quad (20)$$

$$|l_{8-6}| = v_8 \cdot \Delta p \quad (21)$$

where P_{cp} is the compressor power, h_2 and h_1 are the specific enthalpies at the exit and inlet of the compressor. P_{p1} is the power of the defrost liquid refrigerant circulation pump and v_8 is the specific volume of refrigerant after the evaporator exit on the defrost loop.

$$COP_{with\ pump} = \dot{Q}_0 / (P_{cp} + P_{p1}) \quad (22)$$

$$COP = \dot{Q}_0 / P_{cp} \quad (23)$$

where $COP_{with\ pump}$ represents the COP considering also the power of the defrost liquid refrigerant circulation pump and COP stands for the refrigeration cycle.

Based on the mathematical model presented before by *Arora et al., (2008), Havelsky, (2000), Selbas, et al., (2006),* a program has been developed in Engineering Equation Solver. Data resulted is expressed below for R600a, R600, R290, R32, R404a, R134a, R1234yf and R1234ze(E).

RESULTS

Figure 2 shows that when the defrosting time increases, the mass flow rate of defrosting refrigerant decreases for the same constant amount of ice (m_{ice}=1.4 kg), same evaporating temperature t_0=-30°C and the same quality x_7=0.7 at the exit of the PCMhx. Additionally, when defrost time is 30 minutes, refrigerant R600 displays the smallest refrigerant mass flow rate (0.0013 kg/s), while refrigerant R404A has the highest mass flow rate of roughly (0.0032 kg/s). For the defrosting time of 60 min increases the values of the defrosting refrigerant mass flow rate are much closer to each other compared to a defrosting time of 10 min.

Figure 3 and Table 2 show the COP values in function of the defrosting time for the analyzed refrigerants considering the same t_0=-30°C and quality x_7=0,7.

The coefficient of performance (COP) increases slowly with the increase of the defrosting time. It can be seen that the $COP_{\text{with pump}}$ of the refrigeration system with a PCM based defrosting is lower than the case of the refrigeration system without (COP). This is due to the fact that the power of the pump has a low value (see eq. 21 and eq. 22) which means that for both situations the coefficient of performance shows very close values.

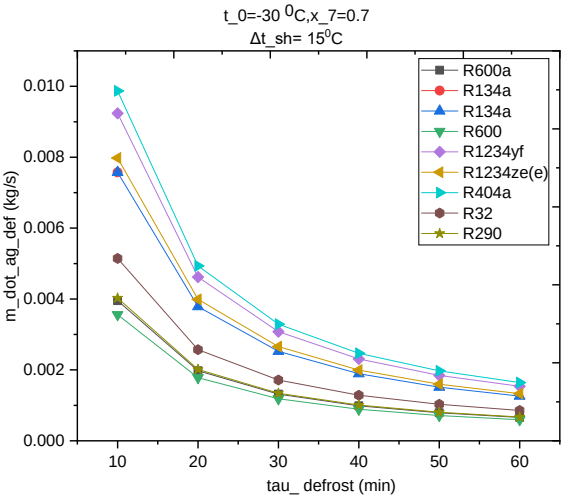

Fig. 2 – Mass flow rate of the defrosting agent versus defrost time

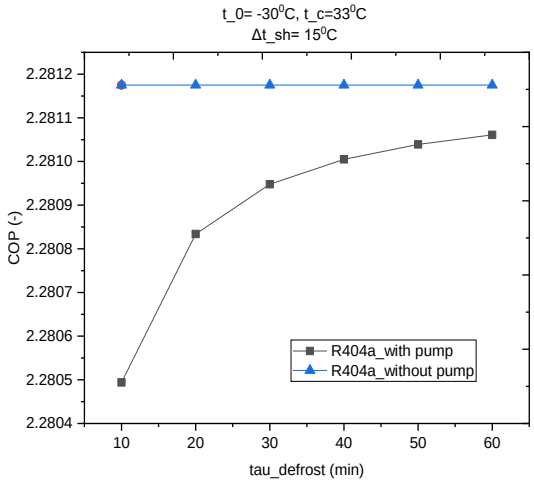

Fig. 3 - Comparison between COP with pump and COP without pump for R404a refrigerant

Table 2

Comparison between COP without pump and $COP_{with\ pump}$ for different refrigerants

Refrigerants	COP	$COP_{with\ pump}$	
		min	max
R600a	2.6743	2.6736	2.6742
R134a	2.6188	2.6182	2.6187
R600	2.7562	2.7556	2.7561
R1234yf	2.4059	2.4052	2.4058
R1234ze(E)	2.5684	2.5678	2.5683
R404A	2.2811	2.2804	2.2810
R32	2.5783	2.5778	2.5782
R290	2.5839	2.5831	2.5838

Table 2 shows that the influence of the defrosting time on the $COP_{with\ pump}$ and COP is the same with the specification that R600 has the highest coefficient of performance and R404A has the lowest for the same operating conditions: t_0=-30°C, t_c=33°C and x_7=0.7.

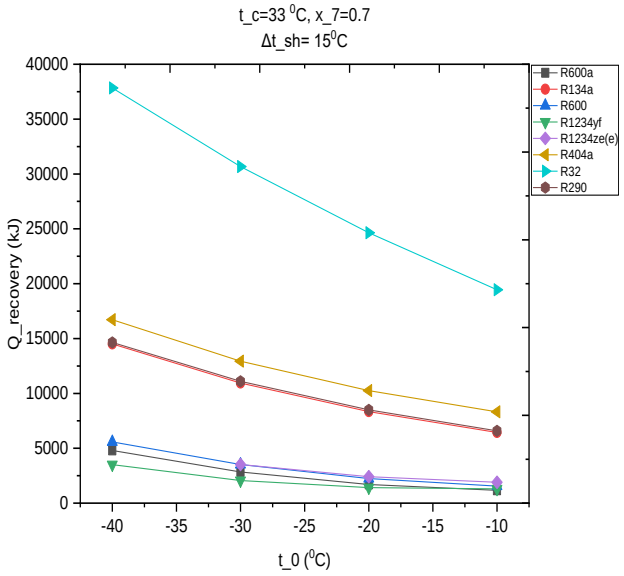

Fig. 4 – Variation of evaporation temperature with PCM heat recovery

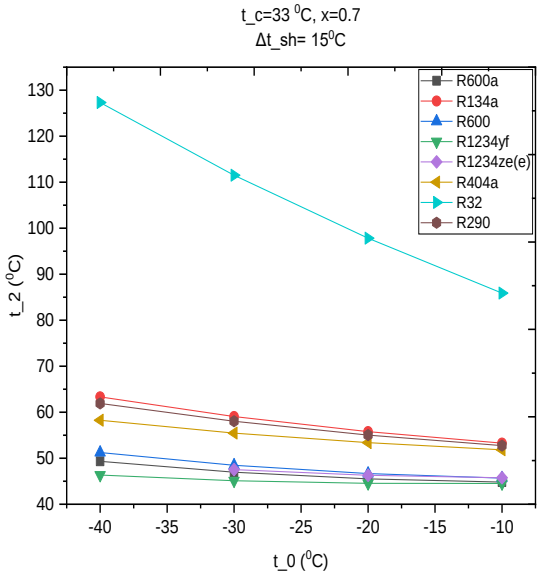

Fig. 5 - The correlation between discharge temperature t_2 and evaporation temperature t_0

Figure 4 shows the variation of the heat which can be recovered ($Q_{recovery}$) from the refrigerant depending on the evaporating temperature (t_0). The figure shows that increasing the evaporating temperature leads to a decrease of the recovered heat. Also, one can notice the heat recovered in the case when the refrigeration system operates at freezing temperatures (-15°C to -40°C) is higher compared to the case when it operates at refrigeration temperatures (-10°C to -15°C). This happen s because when the evaporating temperature decreases the evaporating pressure decreases also which means higher compression ratio and as a result higher compressor discharge temperature t_2 (see Fig.5). It can be noticed that the highest heat recovery value can be achieved for R32 and the lowest one for R1234yf (see Fig.4).

The studied refrigerants fall into 3 groups: R32 with a $Q_{recovery}$ between 20000 kJ and 40000 kJ; R404A, R134a and R290 with a $Q_{recovery}$ between 7000 and 17000 kJ and R1234yf, R1234ze(E), R600 and R600a with a $Q_{recovery}$ between 1000 kJ and 5600 kJ.

As expected, the decrease in evaporating temperature results in an increase in discharge temperature t_2 as in the case of $Q_{recovery}$ (Fig 4). Three groups of refrigerants are distinguished: a) R32, b) R404A, R134a, R290 and c) R600, R600a, R1234yf, R1234ze(E). Group a) is characterized by the highest discharge temperatures (85°C-130°C), group b) between 55°C-65°C and group c) 45°C and 52°C. From the combined analysis of figures 4 and 5, it can be seen that R32 fits best to defrosting with PCM followed by groups b and c.

Table 3

Refrigerant t_c=33°C; x_7=0,7, Δt_{sh}=15°C	Q_{ice} (kJ)		$Q_{recovery}$ (kJ)	
	min(-10°C)	max(-40°C)	min(-10°C)	max (-40°C)
R600a	491,3	579	1165	4801
R134a	491,3	579	6439	14511
R600	491,3	579	1553	5579
R1234yf	491,3	579	1298	3504
R1234ze(E)	491,3	579	1898	3504
R404A	491,3	579	8323	16720
R32	491,3	579	19451	37839
R290	491,3	579	6593	14642

Data specified in Table 3 indicates that, for the operating conditions considered $t_o \in$ [−10◦C, −40◦C], the recoverable heat is sufficient to achieve complete defrosting of the ice accumulated on the evaporator, even if the ice is subcooled and requires a greater amount of heat to melt.

Figure 6 shows that the increase of the condensing temperature t_c leads to an increase in the heat recovery. The influence of the condensing temperature on the recovered heat is different for the 3 groups of refrigerants. In figure 6 it can be observed that for R32 – from group a) and for group b), the increase in the condensing temperature leads to an increase of the heat that can be recovered. For instance, in the case of R32, it doubles from 30000 kJ to 60000 kJ, in case of R404A the increase being even greater. For group c), it can be seen that the recovered heat decreases while condensing temperature increases.

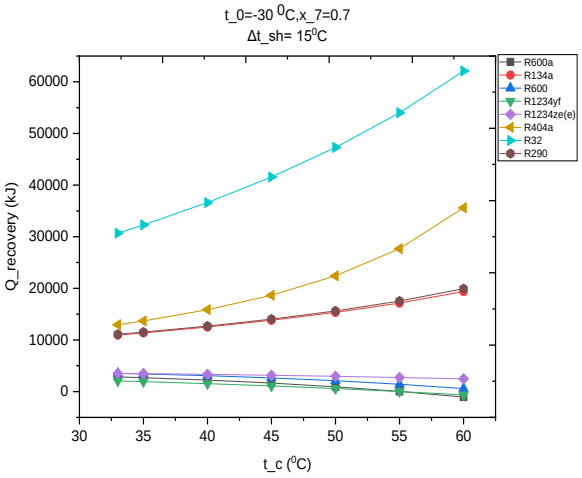

Fig. 6 - Variation of condensing temperature with PCM heat recovery

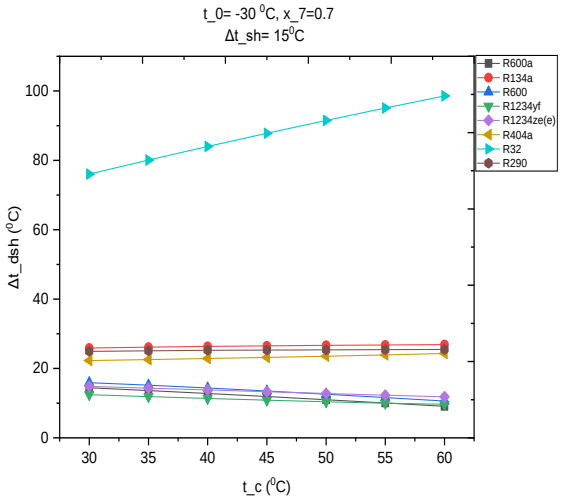

Fig. 7 - Influence of condensing temperature on the degree of desuperheating

According to Figure 7, for refrigerant R32, the desuperheating degree (Δt_{dsh}) increases with the condensing temperature, which justifies the results obtained in the case of heat that can be recovered (Fig. 6). The doubling of $Q_{recovery}$ is not only supported by the increase in Δt_{dsh}, but also by the properties of the refrigerant in terms of enthalpy values (h_2 and h_3). For refrigerants from group b), Δt_{dsh} is quasi-constant and the increase of $Q_{recovery}$ is generated by the enthalpy of the refrigerant. For group c), it is found that $Q_{recovery}$ is correlated with the decrease in Δt_{dsh}. It can be concluded that for certain refrigerants the increase in condensing temperature, in conditions of accumulation of a large amount of ice on the evaporator, can affect defrosting in the version with PCM.

It can be mentioned that the discharge temperature t_2 gives information about the type of PCM that can be used while Δt_{dsh} and $Q_{recovery}$ give information about the maximum amount of heat that can be recovered.

Table 4

Refrigerant t_o=-30°C; x_7=0.7, Δt_{sh}=15°C	Q_{ice} (kJ)	$Q_{recovery}$ (kJ)			
		t_c (°C)	min	t_c (°C)	max
R600a	549.8	60	-1060	30	3036
R134a	549.8	30	10351	60	19377
R600	549.8	60	581.7	30	3648
R1234yf	549.8	60	-640.9	30	2248
R1234ze(E)	549.8	60	2475	30	3576
R404A	549.8	30	11947	60	35608
R32	549.8	30	28419	60	62103
R290	549.8	30	10497	60	19936

Upon careful analysis of Table 4, it is observed that for the group of refrigerants in category c), under tropical condensing temperatures, the recoverable heat decreases. For refrigerants such as R600a and R1234yf, the recoverable heat reaches negative values due to the fact that the refrigerants in category c) are isentropic. Consequently, the compression process leads to a discharge temperature t_2 lower than the condensing temperature, which means a reduction or even elimination of the desuperheating degree required for heat recovery. Under these conditions, it is no longer possible to recover heat from the refrigerant at the compressor discharge for the specified operating parameters.

Table 5

Refrigerant t_0=-30°C; x_7=0.7, Δt_{sh}=20°C	Q_{ice} (kJ)	$Q_{recovery}$ (kJ)			
		t_c (°C)	min	t_c (°C)	max
R600a	549.8	60	4334	30	6443
R600	549.8	60	5329	30	6807
R1234yf	549.8	30	6686	60	7934
R1234ze(E)	549.8	30	7344	30	8905

Table 5 presents the results obtained for a 20°C superheating degree. These results show a significant increase in recoverable thermal energy, thereby making PCM-based defrosting feasible for isentropic refrigerants.

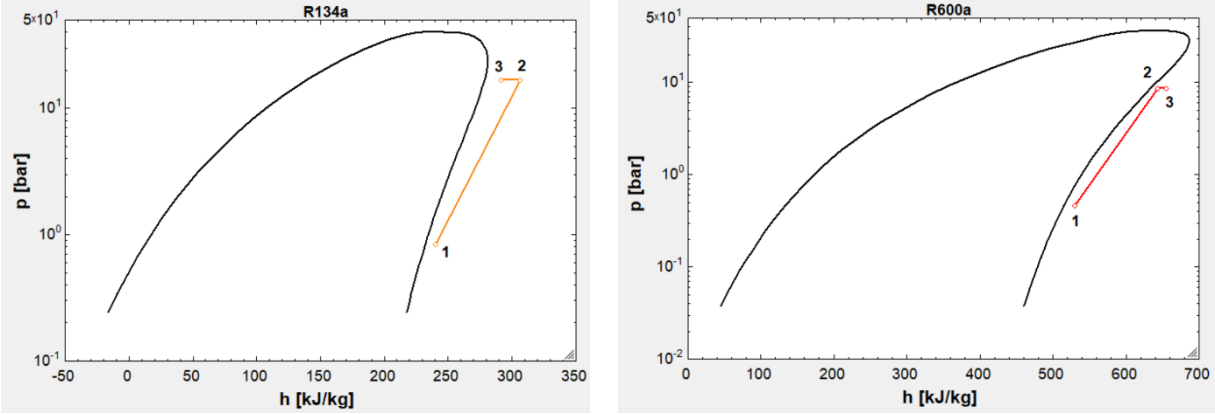

a) b)

Fig. 8 – Compression and recovery processes for wet or dry refrigerants (a) and for isentropic refrigerants (b) in p-h diagram

Figures 8a and 8b illustrate two cases: (a) wet or dry refrigerants (e.g., R134a) and (b) isentropic refrigerants. The refrigerants R32, R404A, R134a, R290 from groups a) and b) are wet or dry. For these refrigerants the enthalpy in state 3 is lower than the enthalpy in state 2 making heat recovery possible. In Figure 8a and 8b the thermodynamic state 2 represents the state of the refrigerant at the compressor discharge and state 3 is the state of the refrigerant at the outlet of PCMhx.

In the case of isentropic refrigerants in group c): R600, R600a, R1234yf, R1234ze(E), the enthalpy of state 2 is lower than the enthalpy of state 3. Under these conditions, the possibility of recovering heat from the refrigerant at the compressor discharge is reduced to zero. Therefore, to enable PCM-based defrosting, it is necessary to increase the superheating degree before the compressor inlet.

Figure 9 shows the influence of the refrigerant quality over $COP_{with\ pump}$. From Figure 9 one can notice that for refrigerant quality values ranging from 0 to 0.1 the $COP_{with\ pump}$ increases abruptly and for values between 0.2 and 1 it increases much slower. The increase in $COP_{with\ pump}$ is attributed to the high-power input required by the liquid circulation pump during the initial phase of the defrosting process. As the liquid refrigerant circulates through the evaporator, its condensation rate progressively decreases, resulting in a gradually reduced flow rate of liquid refrigerant. Consequently, the power required to drive the pump decreases, leading to a slight yet linear increase in the $COP_{with\ pump}$.

Table 6 shows the effect of refrigerant quality on $COP_{with\ pump}$. It can be noticed that the refrigerant quality has a small impact on $COP_{with\ pump}$ and at the same time refrigerant R600 has the highest value out of all refrigerants analyzed in the present study. In Table 6 a higher number of digits have been used to point out the influence of the refrigerant quality (x_7) at the exit of the PCMhx on the $COP_{with\ pump}$. The influence of quality x_7 on $COP_{with\ pump}$ is not very strong and can be noticed after several digits depending on the refrigerant.

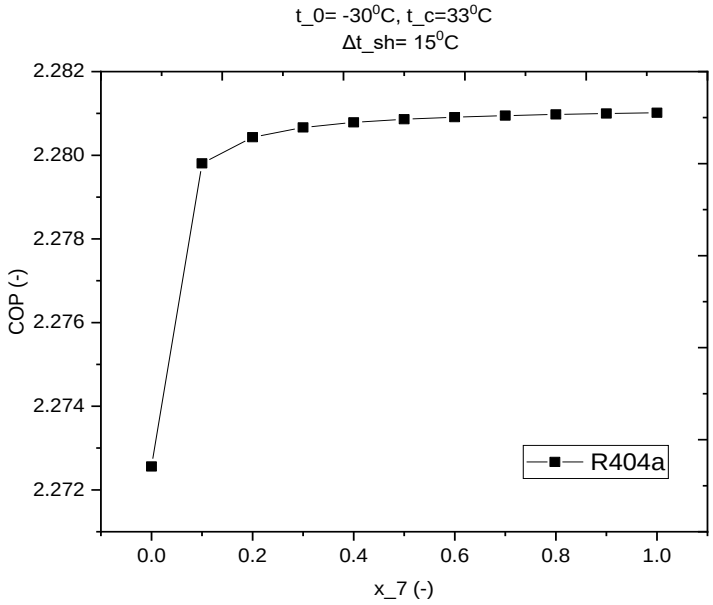

Fig. 9 - Influence of refrigerant quality over $COP_{with\ pump}$

Table 6

x_7	$COP_{with\ pump}$							
	R600a	R134a	R600	R1234yf	R1234ze(E)	R404A	R32	R290
0	2.6698	2.6122	2.7527	2.4000	2.5633	2.2725	2.5654	2.5744
0.1	2.6731	2.6176	2.7551	2.4046	2.5672	2.2798	2.5772	2.5822
0.2	2.6736	2.6181	2.7556	2.4052	2.5677	2.2804	2.5777	2.5831
0.3	2.6738	2.6183	2.7558	2.4054	2.5679	2.2806	2.5779	2.5833
0.4	2.6740	2.6184	2.7559	2.4055	2.5680	2.2807	2.5780	2.5835
0.5	2.6740	2.6185	2.7559	2.4056	2.5681	2.2808	2.5781	2.5835
0.6	2.6741	2.6185	2.7560	2.4057	2.5681	2.2809	2.5781	2.5836
0.7	2.6741	2.6186	2.7560	2.4057	2.5682	2.2809	2.5781	2.5836
0.8	2.6741	2.6183	2.7560	2.4057	2.5682	2.2809	2.5781	2.5837
0.9	2.6742	2.6186	2.7561	2.4057	2.5682	2.2809	2.5781	2.5837
1	2.6742	2.6186	2.7561	2.4058	2.5682	2.2810	2.5782	2.5838

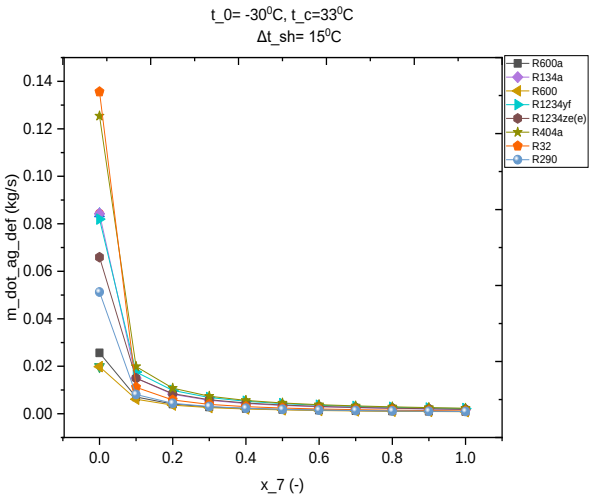

Fig. 10 - Effect of defrost refrigerant mass flow rate on refrigerant quality

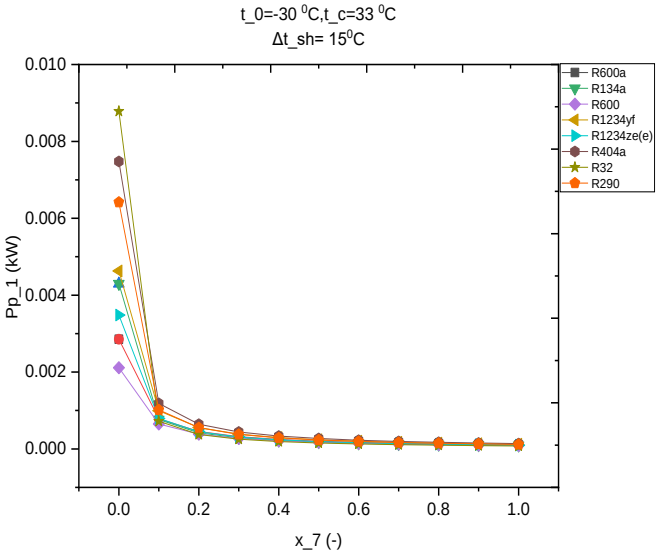

Fig. 11 - The relationship between pump power and refrigerant quality

Figure 10 shows the relationship between the mass flow rate of defrosting refrigerant and refrigerant quality x_7. As expected, there is a significant correlation between these two parameters. The figure demonstrates that as the quality (x_7) increases, the mass flow rate of refrigerant required to maintain the same Q_{ice} decreases. This means that with a decrease in the mass flow rate of defrosting refrigerant the quality increases. Furthermore, the value of x_7 has an influence on the heat transfer from the PCMhx as well as on the power input of the pump, as shown in Figure 11.

Figure 11 shows the relationship between quality (x_7) and the power input of the defrost refrigerant pump. It shows that as x_7 increases from 0 to 1, the mass flow rate of defrost refrigerant decreases. This decrease leads to an increase in the work required to maintain the same pump power. This explains the fact that $COP_{with\ pump}$ of the refrigeration system with PCM based defrosting increases with the increase of x_7, respectively the decrease of the defrosting refrigerant mass flow rate.

CONCLUSIONS

In this paper, the effect of using PCM heat storage for defrosting the evaporator of a refrigeration system was studied using different refrigerants. The impact of various refrigerants and system parameters on the energy performance of PCM-based defrosting was investigated under the same working conditions.

It was observed that as the defrosting time increases, the refrigerant flow rate required for PCM-based defrosting decreases. Among the refrigerants analyzed, R600 exhibited the lowest mass flow rate, while R404A the highest in order to defrost the same mass of ice.

Additionally, the $COP_{with\ pump}$ of the refrigeration system with PCM-based defrosting increases gradually with defrosting time, but it remains slightly lower than the system without defrosting, having comparable values in both cases.

The results indicate that an increase in the evaporating temperature leads to a decrease in the recoverable heat. However, for evaporating temperatures between -10°C and -40°C, the recoverable heat is sufficient to achieve complete defrosting of the ice accumulated on the evaporator.

In contrast, an increase in the condensing temperature improves the amount of recoverable heat for dry and wet refrigerants such as R32, R404A, R134a, and R290, but reduces it for isentropic refrigerants, including R600a, R600, R1234yf, and R1234ze(E).

Superheating plays a critical role in enhancing heat recovery. A higher superheating degree of significantly increases the recoverable heat, making PCM-based defrosting viable for isentropic refrigerants. Contrarily, the desuperheating degree varies with condensing temperature: it increases for R32, remains nearly constant for group b) refrigerants, and decreases for group c) refrigerants. This suggests that increasing the condensing temperature can influence the defrosting process differently depending on the refrigerant.

Previous analysis reveals that R32 is the most suitable refrigerant for PCM-based defrosting, followed by refrigerants in groups b) and c).

Additionally, the refrigerant quality at state 7 has a minimal influence on $COP_{with\ pump}$, with the highest value recorded for R600. As the refrigerant quality increases, the refrigerant mass flow rate required for defrosting decreases, resulting in lower power input for the circulation pump.

ACKNOWLEDGEMENT

This research was funded by the Romanian Ministry of Education and the National University of Science and Technology POLITEHNICA Bucharest through the PubArt Programme.

REFERENCES

[1] Al Douri Jamal, Apostol V., Pop H., Prisecaru T., Pavel C.C., Uta I., Ioniță C., Popa L. (2023), Improving performance of cold room refrigeration system by desuperheating energy recovery using PCMs, *INMATEH - Agricultural Engineering*, Vol. 70 pp.549-556. DOI: https://doi.org/10.35633/inmateh-70-53

[2] Al-Douri Jamal. (2024). Comparison between defrosting methods using different refrigerants, *U.P.B Scientific Bulletin*, Vol. 86, pp. 80-94.

[3] Amer M., Wang C.C. (2017). Review of defrosting methods, Renewable and Sustainable *Energy Reviews*, Vol. 73(C), pp.53-74. DOI: 10.1016/j.rser.2017.01.120

[4] Arora A., Kaushik S.C. (2008). Theoretical analysis of a vapor compression refrigeration system with R502, R404A and R507A. *International Journal of Refrigeration*, Vol.31, pp.998-1005.

[5] Dobre C., Costin M., Constantin M. (2024). A Review of Available Solutions for Implementation of Small–Medium Combined Heat and Power (CHP) Systems. *Inventions.* Vol. 9:82. DOI: 10.3390/inventions9040082
[6] Dong J.K., Jiank Y.Q., Yao Y., Zhang X.D. (2011). Operating performance of novel reverse-cycle defrosting method based on thermal energy storage for air source heat pump. *Journal of Central South University of Technology*, Vol. 18, pp. 2163-2169.
[7] Essadik M., Hajabdollahi Ouderji Z., McKeown A., Lu Y. (2024), A multi-valve flexible heat pump system with latent thermal energy storage, Energy & Buildings, Vol. 321.
[8] Havelský V. (2000) Investigation of refrigerating system with R12 refrigerant replacements, *Applied Thermal Engineering*. Vol.20, Issue 2, pp.133-140.
[9] Hepbasli Arip (2012). Low exergy (LowEx) heating and cooling systems for sustainable buildings and societies. *Renewable and Sustainable Energy Reviews*, Vol. 16, pp. 73-104.
[10] Jin Xin., Wu Fengping., Xu Tao, Huang Gongsheng, Wu Huijun., Zhou Xiaoqing, Wang Dengjia, Liu Yanfeng, Lai Alvin. (2021). Experimental investigation of the novel melting point modified Phase–Change material for heat pump latent heat thermal energy storage application. *Energy*, Vol. 216, 119191.
[11] Kharseh M., Altorkmany, L., Al-Khawaj M., Hassani F. (2014), Warming impact on energy use of HVAC system in buildings of different thermal qualities and in different climates, *Energ. Conver. Manage*, Volume 81, pp. 106-111.
[12] Le Gall R., Grillot J.M., Jallut C. (1997), Modelling of frost growth and densification, *International Journal of Heat and Mass Transfer*, Vol. 40, Issue 13, pp. 3177-3187.
[13] Li Zhi-Ling, Zhang Chun-Lu, Liu Hui-Ming, Wang Xi-Chun. (2024). Feasibility analysis of thermal storage defrosting method for air source heat pump: From energetic and economic viewpoints. *Applied Thermal Engineering*, Vol. 236(D), 121828.
[14] Liu Zhongbao, Li Ao, Wang Qinghua, Chi Yuanying, Zhang Linfei. (2017). Experimental study on a new type of thermal storage defrosting system. *Applied Thermal Engineering*. Vol.118, pp.256-265. https://doi.org/10.1016/j.applthermaleng.2017.02.077
[15] Liu Zhongbao, Zhao Fei, Zhang Lingfei, Zhang Ran, Yuan Meng, Chi Yuanying. (2018). Performance of bypass cycle defrosting system using compressor casing thermal storage for air-cooled household refrigerators. *Applied Thermal Engineering*, Vol.130, pp.1215-1223. https://doi.org/10.1016/j.applthermaleng.2017.11.077
[16] Ning Zhaozhong, Zhang Xuelai, Ji Jun, Shi Yao, Du Fulin. (2023). Research progress of phase change thermal storage technology in air-source heat pump. *Journal of Energy Storage*. Vol. 64(5). DOI: 10.1016/j.est.2023.107114
[17] Ragıp Y., Atta U., Akyuz A., Tuncer A.D. (2023). A new approach for environmental analysis of vapor compression refrigeration systems: Environmental impact index, *Thermal Science and Engineering Progress.* Vol. 42, p.101871. 10.1016/j.tsep.2023.101871
[18] Selbaş R., Kızılkan Ö., Şencan A. (2006). Thermoeconomic optimization of subcooled and superheated vapor compression refrigeration cycle, *Energy*, Vol. 31, pp.2108-2128.
[19] Yang B., Dong J., Zhang L., Song M., Jiang Y., Deng S. (2019), Heating and energy storage characteristics of multi-split air source heat. *Applied Energy.* Vol. 238. pp. 303-310.
[20] Zhang Long, Dong Jiankai, Jiang Yiqiang, Yao Yang. (2014). A novel defrosting method using heat energy dissipated by the compressor of an air source heat pump, *Applied Energy*, Vol.133, pp.101-111. https://doi.org/10.1016/j.apenergy.2014.07.039
[21] ****Engineering Equation Solver Academic Professional*, V.10.836-3D #4487, (2020). Faculty of Mechanical Engineering, University POLITEHNICA of Bucharest, Romania.